JAAS

PAPER

View Article Online
View Journal

Cite this: DOI: 10.1039/c7ja00059f

An ICP-MS-based platform for release studies on silver-based nanomaterials

Isabel Abad-Alvaro, Eduardo Bolea, Francisco Laborda* and Juan R. Castillo

Engineered nanoparticles are being incorporated into different products and nanocomposites. The release of these nanoparticles, as well as other derived species, can subsequently lead to consumer and environmental exposure, being a relevant factor for risk assessment. The need for analytical methods for the detection, characterization and quantitation of these released species under relevant conditions becomes evident. In this work, a platform of methods based on the use of inductively coupled plasma mass spectrometry (ICP-MS) is proposed to obtain information about the release of silver from silver based nanocoatings and nanocomposites. The sensitivity and element specific response of conventional ICP-MS is complemented by the use of the technique in single particle mode and in combination with ultrafiltration and asymmetrical flow field flow fractionation. By using these three methods, information about the release of both dissolved and particulate forms of silver, as well as the size of the nanoparticles, can be obtained under a variety of scenarios at concentrations down to 0.1 μg L^{-1} and a nanoparticle diameter of 5 nm. The feasibility of the platform was checked through a number of paradigmatic cases.

Received 13th February 2017
Accepted 20th April 2017

DOI: 10.1039/c7ja00059f

rsc.li/jaas

1. Introduction

There is an increasing need for reliable analytical methods to get information related to engineered nanomaterials (ENMs).[1] The analytical information demanded by stakeholders, government agencies or researchers can range from the detection of nanoparticles to their characterization (size, shape, composition…) or the determination of their concentrations. ENMs are commonly being applied onto surfaces or incorporated into the matrixes of diverse materials; in such cases, additional information about the behaviour of the nanoproduct along its life cycle is also demanded.[2,3] For solid products, this means to be able to monitor under diverse conditions the release of nanoparticles and/or dissolved components, and their interaction with other species, as well as the agglomeration/aggregation of the nanoparticles, or the modification of their surfaces. For inorganic nanomaterials, and depending on the release scenario, this can imply to cope with pristine or surface modified nanoparticles, as well as ionic or complexed species from the dissolution/oxidation of the original nanoparticles.

There is currently no single analytical method able to detect, characterize, and quantify nanoparticles in complex systems. Thus a multimethod approach is often required to obtain the analytical information demanded.[4] On the other hand, although a wide range of analytical techniques is available to study ENMs, limitations become evident when they are applied to the analysis of ENMs in complex samples, like those from environmental or biological systems, at realistic concentrations. Focusing on inorganic nanoparticles, the use of element-specific techniques is the most valuable tool for their detection. Due to the low detection limits attainable (down to ng L^{-1}), inductively coupled plasma-mass spectrometry (ICP-MS) is one of the most used techniques for detection, as well as for quantification, of the element/s present in the nanoparticles and the sample.[5] Conventional ICP-MS is sensitive to the elements present in a sample that contains a nanomaterial, but it is not capable of providing any information about the physicochemical form of the element (*e.g.*, if present as dissolved species or as particulate), or any other information related to the nanoparticles (size, shape, aggregation…). When ICP-MS is combined with a previous separation step, like ultracentrifugation,[6] ultrafiltration,[7] cloud point[8] or solid phase extraction,[9] additional information about the released soluble species or the nanoparticles themselves can be obtained. On the other hand, the use of ICP-MS as an element-specific detector, on-line coupled to continuous separation techniques, like field flow fractionation (FFF)[10] or hydrodynamic chromatography (HDC)[11] allows us to obtain information about the size of the nanoparticles separated, as well as quantitative information with respect to their size. Finally, when ICP-MS is used in single particle mode (SP-ICP-MS) it is possible to detect and quantify

Group of Analytical Spectroscopy and Sensors (GEAS), Institute of Environmental Sciences (IUCA), University of Zaragoza, Pedro Cerbuna 12, 50009 Zaragoza, Spain. E-mail: flaborda@unizar.es

dissolved *versus* particulate forms of the element in the same sample, and provide information about the mass of the element per particle and its size (if additional information about shape, composition and density of the particles is available), as well as about its number and mass concentration at levels below ng L^{-1}.[12]

Silver-based nanomaterials are used in a wide range of products due to their antimicrobial properties.[13] The biocidal activity of these nanomaterials is based on the release of metallic silver nanoparticles, as well as silver(I) due to oxidation processes.[14] Thus information about silver release cannot be limited to total concentrations and detailed information about both particulate and dissolved silver is needed.[15] Although potentiometric measurements with ion selective electrodes can provide information about dissolved silver in ionic form (Ag^+), the use of ultrafiltration in combination with an atomic spectrometric technique like ICP-MS allows us to get information about silver species with size/molecular mass below the cut-off of the ultrafiltration membrane. In this context, small pore size membranes (1–5 kDa) are commonly used for the isolation of ionic silver and low molecular mass complexes.[16,17] A number of continuous separation techniques coupled to ICP-MS, including reversed phase chromatography[18] and capillary electrophoresis,[19] have proved to be suitable for the simultaneous separation of silver(I), as well as silver nanoparticles, although the developed methods have been checked just as proofs-of-concept. Alternatively, asymmetrical flow field flow fractionation (AF4) allows us to obtain information about silver complexes not filtered through the permeable membrane of the separation channel, and silver nanoparticles.[20,21] By using SP-ICP-MS, quantitative information about any form of dissolved and particulate silver species can be obtained, in addition to mass per particle/size information.[22] Alternatively, AF4 has been coupled to ICP-MS working in single particle mode, both off-line[23] and on-line,[24] to differentiate silver nanoparticles with similar hydrodynamic sizes.

The aim of this work is to show, through a number of cases, the feasibility of a platform of analytical methods based on the use of ICP-MS to get different types of complementary information demanded to solve real problems related to release studies involving silver-based nanomaterials. The methods selected were: (i) ultrafiltration in combination with ICP-MS, for the determination of the dissolved fraction (smaller than the membrane pore size) of the element; (ii) single particle ICP-MS, to detect the presence of dissolved and particulate forms of the element; (iii) asymmetrical flow field flow fractionation (AF4) coupled to ICP-MS, to obtain information about the size of the nanoparticles and their mass concentration.

2. Experimental

2.1. Instrumentation

A Perkin-Elmer Sciex model ELAN DRC-e ICP mass spectrometer (Toronto, Canada) was used throughout. The sample introduction system consisted of a glass concentric Slurry nebulizer and a baffled cyclonic spray chamber (Glass Expansion, Melbourne, Australia). Default instrumental and data acquisition parameters are listed in Table 1.

Table 1 Default instrumental and data acquisition parameters of ICP-MS

Instrumental parameters		
RF power		1200 W
Argon gas flow rate		
Plasma		15 L min^{-1}
Auxiliary		1.2 L min^{-1}
Nebulizer		1.0 L min^{-1}
Sample uptake rate		1.0 mL min^{-1}
Data acquisition parameters		
Measuring mode	Standard	Single particle detection
Points per spectral peak	1	1
Sweeps	20	1
Dwell time	50 ms	5 ms
Readings per replicate	1	12 000
Settling time	3 ms	3 ms
Integration time	1 s	60 s
Isotopes monitored	$^{107}Ag^{109}Ag$	

The AF4 system used was an AF2000 (Postnova Analytics, Landsberg, Germany). The trapezoidal channel was 27.5 cm in length and from 2 to 0.5 cm in width, and the spacer used for all the measurements was 350 mm thick. An ultrafiltration membrane of polyether sulfone (PES) (cut-off 5 kDa; PostnovaAnalytics) was used as the accumulation wall.

2.2. Chemicals

Diluted suspensions of silver nanoparticles were prepared from commercially available suspensions. Suspensions of monodisperse silver nanoparticles of 10 (PlasmaChem, Berlin, Germany), 20 ± 5, 40 ± 5, 60 ± 5 and 100 ± 8 nm (Sigma-Aldrich Chemie, Buchs, Switzerland) were used. Dilutions were prepared in ultrapure water (Milli-Q Advantage, Molsheim, France) by accurately weighing (±0.1 mg) aliquots of the stock suspensions after one minute sonication. After dilution and before each analysis, the suspensions were sonicated for one minute.

Aqueous silver solutions were prepared from a standard stock solution of 1000 mg L^{-1} (Panreac, Barcelona, Spain) by dilution in ultrapure water. The carrier used for AF4 separation was prepared by dissolving the corresponding mass of sodium dodecyl sulphate (SDS) (BioRad, California, USA) in ultrapure water.

2.3. Materials

Two types of nanomaterials were studied: glass slides coated with silver nanoparticles and structured SiO_2-based nanocomposites containing a single layer of silver nanoparticles.

Glass slides (75 × 25 cm) were coated directly with silver nanoparticles by plasma vapour deposition, producing a porous nanostructured thin film. Structured nanocomposites (SiO_2/AgNPs/SiO_2/Si) consisted of squared plates (2 × 2 cm), where a single layer of AgNPs was embedded in a 90 nm thick silica layer by a combination of physical vapour deposition and plasma-enhanced chemical vapour deposition.

Table 2 AF4 cross-flow programs. Out flow: 1.00 mL min^{-1}

Program step		Time (min)	Cross-flow	
			Mode	mL min^{-1}
Injection/focusing	Injection flow 0.2 mL min^{-1}	5		1
Separation	Program 1[a]	7	Constant	0.500
		1	Linear decay	0.500 to 0
		2	Constant	0
	Program 2[b]	8	Constant	0.325
		1	Linear decay	0.325 to 0
		2	Constant	0

[a] Nanocoated glass slides. [b] Structured SiO_2-based nanocomposites.

2.4. Procedures

2.4.1. Silver release experiments. Glass slides coated with silver nanoparticles were put into polyethylene tubes, filled with 50 mL of ultrapure water and placed in a rotary tumbler for 24 hours at 29 rpm and room temperature in darkness. After this period, the suspension from the release assays was transferred to a polyethylene tube and stored at 4 °C in darkness for analysis.

In the case of nanocomposites, plates containing the embedded silver nanoparticles were immersed in 6 mL of 10 mM 3-morpholinopropane-1-sulfonic acid (MOPS) adjusted at pH 7.5 and shaken for 20 hours at room temperature in darkness. After removing the plate, algae (*Chlamydomonas reinhardtii*) were added to 3 mL of the solution to get a cell concentration of 6×10^5 cells per mL. After 1 hour of algae exposure under agitation and continuous illumination to avoid aggregation and ensure normal activity of algae, the medium was centrifuged and the supernatant was stored at 4 °C in darkness for analysis. Control plates with no embedded silver nanoparticles were also tested under the same conditions.

2.4.2. Ionic silver determination by ultrafiltration and ICP-MS. The dissolved silver in the suspensions was isolated by removing silver nanoparticles using Nanosep Pall centrifugal ultrafilter devices with cut-off membranes of 3 kDa (equivalent to a 2 nm hydrodynamic diameter). Ultrafilter devices were washed by centrifugation with 500 μL of ultrapure water twice. The second washing was kept to check for any potential contamination. Suspensions were sonicated for two minutes; 500 μL were subjected to centrifugation for 20 min at 9000 rpm and 20 °C (Thermo Heraeus Multifuge X1R, equipped with a fixed angle rotor for Eppendorf tubes, Walthman, USA). The ultrafiltrate (*ca.* 500 μL) was diluted up to 5 mL with ultrapure water prior to ICP-MS analysis.

2.4.3. Silver nanoparticle determination by AF4-ICP-MS. 100 μL of the suspensions were injected directly in the AF4 channel. A 0.01% (m/v) SDS solution prepared in ultrapure water adjusted to pH 8.0 was used as the carrier for separation and size characterization of silver nanoparticles. The cross-flow programs listed in Table 2 were used.

2.4.4. SP-ICP-MS measurements. The suspensions were diluted with ultrapure water, according to the silver concentration, and measured in single particle mode, using a dwell time of 5 ms with an integration time of 60 s (12 000 points). The limited data acquisition rate of the instrument was overcome by monitoring two isotopes (^{107}Ag and ^{109}Ag) and using the settling time of the quadrupole to empty the buffer. Although the use of dwell times in the millisecond range may lead to record nanoparticle events as split events or as 2 or more nanoparticle events,[25] these effects can be minimized by appropriate data processing[26] or by selecting the adequate nanoparticle concentration.[27] For the samples analysed in this work, this was not a serious limitation because SP-ICP-MS measurements were used for screening purposes.

2.4.5. Silver determination by ICP-MS. Suspensions from the release studies with the glass slides were directly quantified, whereas suspensions from structured SiO_2-based nanocomposites were diluted 1 : 10 with ultrapure water prior to the ICP-MS analysis.

3. Results and discussion

3.1. Performance of the ICP-MS based methods

Although concentration is not a serious limitation in SP-ICP-MS, because number concentration detection limits of 1000 mL^{-1} can be achieved with the conditions used in this work,[28] size detection limits are conditioned by the background levels and the occurrence of dissolved species of the element being measured. Size detection limits, calculated by using the 3σ criterion,[29] of 24 nm were achieved in ultrapure water, whereas they increased up to 40 nm in the presence of 135 ng L^{-1} of Ag(I).

The achievable sensitivity of the ultrafiltration method combined with the determination of silver in the ultrafiltrate by ICP-MS depends on the volumes and dilution selected. Following the procedure describe in Section 2.4.2, detection limits of 100 ng L^{-1} were calculated from the ultrafiltration blanks. By using the ultrafiltration membranes with a cut-off of 3 kDa, the ultrafiltrate can contain silver bearing nanoparticles below *ca.* 2 nm and silver(I) species below 3 kDa, including ionic Ag^+ if no silver complexing ligands are present.

With respect to AF4-ICP-MS, nanoparticles from *ca.* 5 nm could be separated using the nanoparticle programs summarized in Table 2. Concentration detection limits were calculated as three times the standard deviation of the baseline divided by the sensitivity.[21] 100 μL of a diluted suspension of 10-nm Ag NP standard (50 μg L^{-1} silver concentration) was injected. The peak

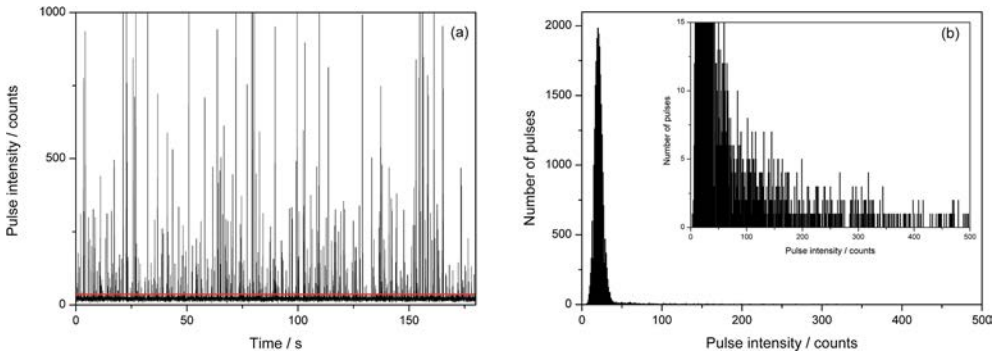

Fig. 1 Analysis of a suspension from a release assay with a silver nanocoated slide by SP-ICP-MS. (a) Time scan of the suspension containing dissolved and particulate silver. (b) Pulse intensity frequency histogram of data from (a). Red line: 3σ threshold.

height at the maximum of the ICP-MS fractogram obtained was used for calculations. A value of 0.1 μg L^{-1} was found, which corresponds to a concentration of 1.8×10^{10} L^{-1} for silver nanoparticles of 10 nm.

3.2. Case studies

Two case studies were selected to show the feasibility of the proposed ICP-MS platform to obtain information about the fate and occurrence of different silver species released from a material containing silver nanoparticles in contact with an aqueous phase. Although the first case study is a paradigmatic example, involving the release of silver into ultrapure water, the second one corresponds to a typical ecotoxicological test, where the released silver interacts with algae, increasing the complexity of the medium.

3.2.1. Case 1: release of silver from a nanocoating. Once the release experiment described in Section 2.4.1 was finished, the glass slide was removed from the suspension and the remaining silver was dissolved with concentrated nitric acid. Silver was measured in this solution and in the suspension by ICP-MS to determine the total silver content of the coating and the total silver released respectively. The total silver content in the coating was 14.02 ± 0.05 μg, whereas 0.82 ± 0.02 μg of Ag was found in the suspension, accounting for 5.8% of the total amount of silver in the coating.

Fig. 1a shows the time scan obtained from the diluted suspension analysed by SP-ICP-MS. The scan showed a baseline at intensities higher than the corresponding blank, indicating the occurrence of dissolved forms of silver. On the other hand, the presence of pulses over the 3σ threshold confirmed the occurrence of silver bearing particles. In SP-ICP-MS, it is a common practice to process raw data from time scans by plotting the pulse intensity *vs.* the pulse intensity frequency, to obtain frequency histograms where the first distribution is due to the background and/or the presence of dissolved forms of the element measured and the second to the particles themselves.[12] Fig. 1b shows the corresponding histogram where just one tailed distribution was present, suggesting that most of the particulate silver corresponds to nanoparticles below the size detection limit[22] (*ca.* 40 nm) which was affected by the presence of dissolved silver. Thus the occurrence of dissolved silver and small silver nanoparticles was prevented to take full advantage of SP-ICP-MS, being restricted to be used as a screening method to confirm the presence of both dissolved and particulate silver.

Because dissolved and particulate silver distributions were not fully resolved in the SP-ICP-MS histograms, quantification of both species was not possible. As an alternative, dissolved silver was fractionated by ultrafiltration and quantified by analysis of the ultrafiltrate by ICP-MS. Table 3 summarizes the corresponding results, confirming the qualitative information obtained by SP-ICP-MS about the occurrence of dissolved and particulate silver, which accounted for the 43% and 57%, respectively, of the total silver released. Due to the use of the lower pore size membrane available and the release medium used, the ultrafiltered silver could be associated with ionic silver (Ag^+), although the occurrence of very small nanoparticles below *ca.* 2 nm may not be discarded. In more complex media, the presence of dissolved Ag(I) forms different than Ag^+, namely those complexed by different ligands, could invalidate the ultrafiltration procedure depending on the molecular mass of the complexes. In any case, the retention of the ionic silver in the membranes used can be considered negligible, with recoveries of 102 ± 3%.[30]

Table 3 Total and fractionated silver released from a nanocoating

Fraction	Technique	Ag (μg)	Ag *vs.* total released (%)
Total Ag	ICP-MS	14.02 ± 0.05	
Total Ag released (AgNP + Ag^+)	ICP-MS	0.82 ± 0.02	
Ag^+ released	UF + ICP-MS	0.35 ± 0.01	42.7 ± 1.1
AgNP released	AF4-ICP-MS	0.47 ± 0.03	57.4 ± 3.8

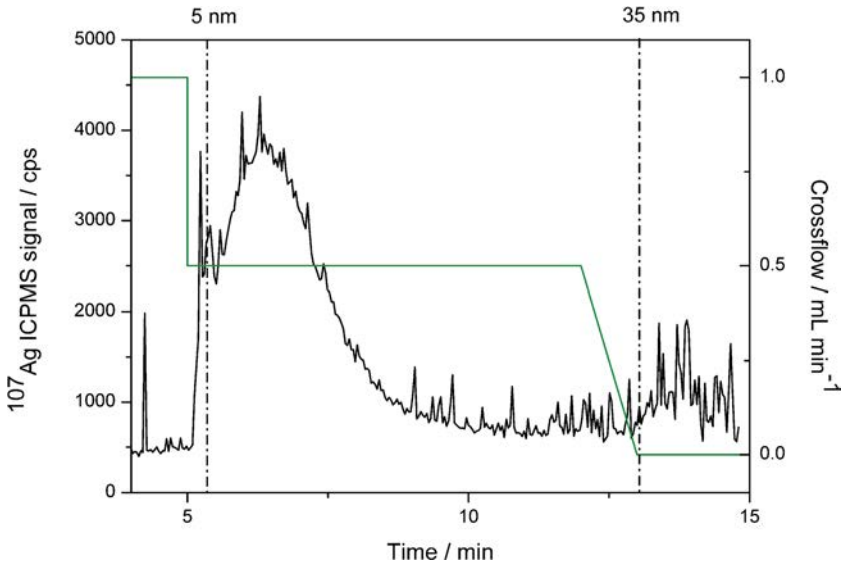

Fig. 2 AF4-ICP-MS fractogram of the suspension from a release assay with a silver nanocoated slide.

The limitations of SP-ICP-MS discussed above to characterize and quantify the silver nanoparticles in the suspension could be overcome by using AF4 coupled to ICP-MS. To this end, the suspension was analysed by AF4-ICP-MS under the conditions described in Section 2.4.3 and Table 2. Fig. 2 shows the corresponding fractogram. Size characterization was done by calibrating the AF4 system *vs.* Ag NP size standards. The following linear relationship between the logarithm of the retention ratio R (elution time corresponding to the void volume divided by the retention time for a given particle) and the logarithm of the diameter (d) in nanometres was experimentally found: $\log R = -0.4507 \log d + 0.3041$ ($r = 0.988$). According to this expression, the separation range using the cross-flow program summarized in Table 2 was 5–35 nm, and the size corresponding to the maximum of the peak was 7.0 ± 0.1 nm. This result justifies the failure of SP-ICP-MS to characterize the silver nanoparticles in the suspension.

The silver nanoparticles were quantified directly from the fractogram against ionic silver standards, injected in flow injection mode, by integrating the fractogram and the flow injection peaks. The silver present as nanoparticles in the suspension was 0.47 ± 0.03 μg, which is in agreement with the particulate fraction determined as the difference between the total silver released and the ultrafiltered silver (0.47 ± 0.02 μg). On the other hand, the recovery of the sample in the AF4 channel was $54 \pm 7\%$, in agreement with the measured content of particulate silver determined by ultrafiltration, which accounted for 57% of total silver, and the loss of dissolved silver through the accumulation wall of the channel.

3.2.2 Case 2: release of silver from a nanocomposite in an ecotoxicological test. Table 4 summarizes the results obtained for the content of total silver in the test media analysed. Different control samples, consisting of test media (10 mM MOPS) from tests performed with or without substrate and with or without algae, were also run (in the absence of silver nanocomposites). Silver concentrations below 0.35 μg L^{-1} were obtained in all cases. Test media from positive assays with silver nanocomposites but not exposed to algae showed higher silver concentrations than those exposed to algae. Because the difference was statistically significant, it suggested that part of the silver released was sorbed by the algae.

The test media were diluted 1 : 1000 and analysed by SP-ICP-MS. Fig. 3 shows the time scans corresponding to samples S2-110 and S2-111. As in the previous case, the occurrence of significant amounts of dissolved silver and the small size of the silver nanoparticles hindered us from fully exploiting the capabilities of SP-ICP-MS, just allowing to screen the release of silver bearing particles along with dissolved silver.

Test media from positive assays were ultrafiltered through 3 kDa membranes and analysed by ICP-MS, confirming the

Table 4 Total and ultrafiltered silver concentration in test media from ecotoxicological tests with *Chlamydomonas reinhardtii*

Sample	Substrate	Algae	Fraction	Silver concentration (μg L^{-1})
Controls				
C1-000	✗	✗	Total	0.02 ± 0.02
C2-000	✗	✗	Total	0.17 ± 0.02
C3-001	✗	✓	Total	0.35 ± 0.03
C4-001	✗	✓	Total	0.25 ± 0.04
C5-100	✓	✗	Total	0.35 ± 0.03
C6-101	✓	✓	Total	0.06 ± 0.03
Substrates with Ag NPs				
S1-110	✓	✗	Total	28.35 ± 1.93
			Ultrafiltered	22.44 ± 1.83
S2-110	✓	✗	Total	37.30 ± 1.57
			Ultrafiltered	25.02 ± 1.93
S1-111	✓	✓	Total	17.30 ± 0.17
			Ultrafiltered	5.72 ± 0.08
S2-111	✓	✓	Total	17.55 ± 0.18
			Ultrafiltered	8.53 ± 0.43

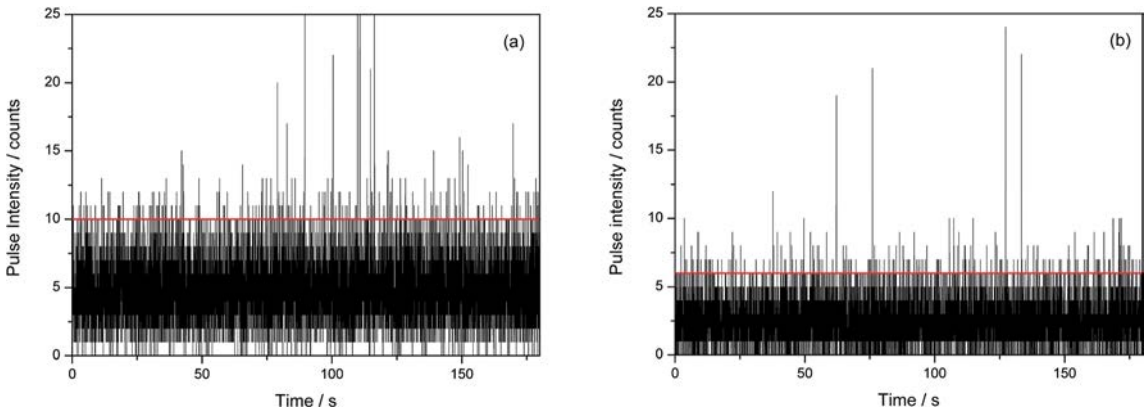

Fig. 3 Analysis of test media from ecotoxicological tests of Ag nanocomposites by SP-ICP-MS. (a) Time scans from test media in the absence (a) and presence of algae (b). Red line: 3σ threshold.

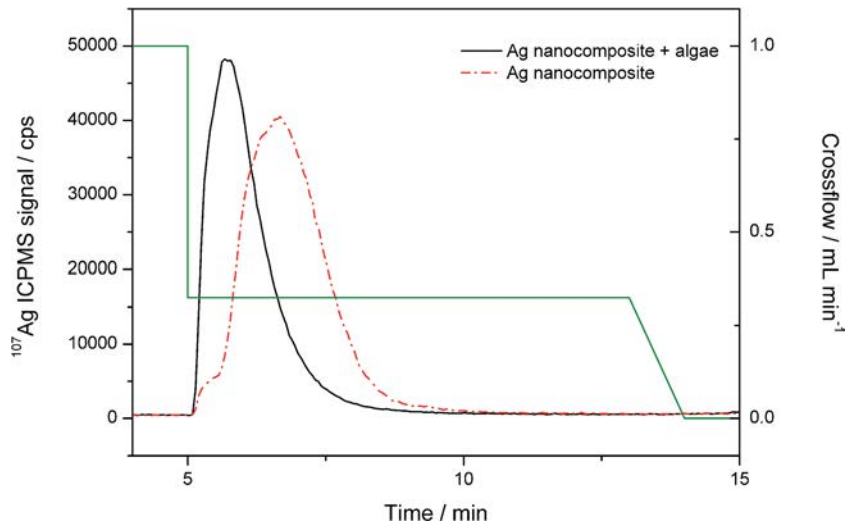

Fig. 4 AF4-ICP-MS fractograms of ecotoxicological test media of Ag nanocomposites in the absence and presence of algae.

occurrence of dissolved silver species below this molecular mass, as summarized in Table 4. Whereas in the assays performed without algae, the fraction of ultrafiltered silver accounted for 73 ± 8% of the total silver released, and it was reduced to 41 ± 11% in the presence of algae. In the absence of algae, the ultrafiltered silver could be associated with ionic silver, because MOPS does not complex silver(I); however, the complexation of silver(I) by algal exopolymeric substances (EPSs) could not be discarded in samples S1-111 and S2-111. In such cases, the occurrence of silver complexed by macromolecules over 3 kDa invalidates the fractionation of dissolved/particulate silver obtained by ultrafiltration, since both silver nanoparticles and silver–macromolecule complexes (>3 kDa) are retained by the membrane.

In comparison with ultrafiltration, AF4 provides a continuous separation of species with respect to their molecular mass/size. Fig. 4 shows the fractograms from samples S2-110 and S2-111, corresponding to ecotoxicological tests performed in the absence and presence of algae. In the first case, a peak partially resolved from the void peak was obtained at 6.7 min, corresponding to 9.2 ± 0.3 nm by calibration against silver nanoparticles. However, in the presence of algae, silver was eluted at 5.7 min, suggesting the occurrence of smaller silver nanoparticles or silver(I) complexes with algal EPSs. Because of the low concentration of silver, the presence of silver nanoparticles could not be confirmed by monitoring the UV-visible absorption at *ca.* 400 nm due to their plasmon resonance, although the UV-visible spectrum at 5.7 min showed a shoulder at 256 nm, typical of organic matter.

To confirm the identity of the peaks, aliquots of the control sample C4-001 (MOPS test medium exposed to algae but not to the silver nanocomposite) were spiked with $AgNO_3$ and 10 nm silver nanoparticles. When the control sample containing algal EPSs was spiked with Ag(I) a peak at 5.9 min was observed, whereas it appeared at 6.6 min when spiked with silver nanoparticles (Fig. 5). Thus although the occurrence of silver nanoparticles below 10 nm could not be discarded, most of the silver released from the nanocomposite during the ecotoxicological

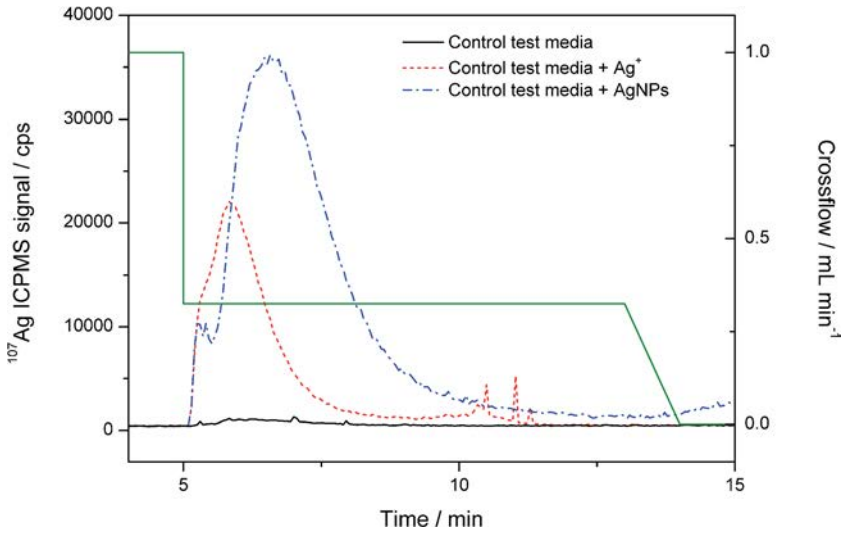

Fig. 5 AF4-ICP-MS fractograms of the control ecotoxicological test media exposed to algae but not to Ag nanocomposites, and spiked with 60 μg L^{-1} of silver as $AgNO_3$ and 10 nm silver nanoparticles.

test was found complexed with algal EPSs, which contributed to the oxidation of the formerly released silver nanoparticles.

4. Conclusions

Release studies of silver-based nanomaterials can involve the detection of both dissolved and particulate forms of silver, their quantification and the size characterization of the released particles. Depending on the complexity of the releasing medium, the dissolved silver can be found as ionic silver(I) (Ag^+) or complexed by ligands present in the medium. Whereas electron microscopy and light scattering techniques can cope with particulate forms at mg L^{-1} levels, for lower concentrations and for dissolved forms, other techniques and methods must be considered. The use of ICP-MS in single particle mode, as well as the combination of conventional ICP-MS with ultrafiltration and AF4, has proven to be a useful approach to obtain the maximum amount of information about the release of silver from a solid nanomaterial under different conditions. SP-ICP-MS could just be used as a screening tool because of the small size of the nanoparticles involved and the presence of dissolved forms of silver(I). More information (size, mass and number concentration) may be obtained when bigger particles are involved or more sensitive instruments are available. In any case, the occurrence of both dissolved and particulate forms of silver was confirmed in the two case studies presented. Ultrafiltration was useful when silver was present in ionic form and not complexed by ligands bigger than the ultrafiltration membrane cut-off, as in the ecotoxicological test case-study, where the amount of dissolved silver(I) was underestimated due to its complexation with algal extracellular polymeric substances. Finally, although AF4-ICP-MS does not provide information about dissolved species of low molecular weight (below the cut-off of the accumulation membrane), both size (hydrodynamic diameters) and quantitative information can be obtained for particles and macromolecular silver species, complementing the two other methods.

The proposed platform of analytical methods based on the use of ICP-MS is a competitive tool for detection, size characterization and quantitation of silver nanoparticles and dissolved silver(I) species, not only in release studies but in other samples containing these species. Although the presented case-studies involved silver, the platform is suitable for being applied to other elements and nanoparticles.

Acknowledgements

This work was supported by the Spanish Ministry of Economy and Competitiveness and the European Regional Development Fund, project CTQ2015-68094-C2-1-R (MINECO/FEDER). The authors would like to acknowledge the use of Servicio General de Apoyo a la Investigación-SAI, Universidad de Zaragoza, for ICP-MS measurements; N. Manninen and A. Cavaleiro (SEG-CEMUC, University of Coimbra), and S. Carvalho (GRF, University of Minho) for providing the silver coated samples; A. Pugliara, R. Carles and C. Bonafos (CEMES CNRS, University of Toulouse), K. Makasheva (LAPLACE, University of Toulouse) and E. Navarro (IPE, CSIC), for providing the culture media for ecotoxicological tests with silver nanocomposites.

References

1 C. Contado, *Front. Chem.*, 2015, **3**, 48.
2 A. Caballero-Guzman and B. Nowack, *Environ. Pollut.*, 2016, **213**, 502–517.
3 A. Mackevica and S. Foss Hansen, *Nanotoxicology*, 2016, 1–13.
4 F. Laborda, E. Bolea, G. Cepriá, M. T. Gómez, M. S. Jiménez, J. Pérez-Arantegui and J. R. Castillo, *Anal. Chim. Acta*, 2016, **904**, 10–32.
5 P. Krystek, A. Ulrich, C. C. Garcia, S. Manohar and R. Ritsema, *J. Anal. At. Spectrom.*, 2011, **26**, 1701.
6 J. M. Unrine, B. P. Colman, A. J. Bone, A. P. Gondikas and C. W. Matson, *Environ. Sci. Technol.*, 2012, **46**, 6915–6924.

7 L. M. Furtado, M. E. Hoque, D. M. Mitrano, J. F. Ranville, B. Cheever, P. C. Frost, M. A. Xenopoulos, H. Hintelmann and C. D. Metcalfe, *Environ. Chem.*, 2014, **11**, 419–430.
8 J. Liu, J. Chao, R. Liu, Z. Tan, Y. Yin, Y. Wu and G. Jiang, *Anal. Chem.*, 2009, **81**, 6496–6502.
9 L. Li, K. Leopold and M. Schuster, *Chem. Commun.*, 2012, **48**, 9165–9167.
10 B. Meermann, *Anal. Bioanal. Chem.*, 2015, **407**, 2665–2674.
11 A. Philippe and G. E. Schaumann, *PLoS One*, 2014, **9**, 1–9.
12 F. Laborda, E. Bolea and J. Jiménez-Lamana, *Trends Environ. Anal. Chem.*, 2016, **9**, 15–23.
13 G. Franci, A. Falanga, S. Galdiero, L. Palomba, M. Rai, G. Morelli and M. Galdiero, *Molecules*, 2015, **20**, 8856–8874.
14 N. Durán, M. Durán, M. B. de Jesus, A. B. Seabra, W. J. Fávaro and G. Nakazato, *Nanomedicine Nanotechnology, Biol. Med.*, 2016, **12**, 789–799.
15 B. Reidy, A. Haase, A. Luch, K. A. Dawson and I. Lynch, *Materials*, 2013, **6**, 2295–2350.
16 Y.-J. Lee, J. Kim, J. Oh, S. Bae, S. Lee, I. S. Hong and S. H. Kim, *Environ. Toxicol. Chem.*, 2011, **31**, 155–159.
17 A. Ozaki, E. Kishi, T. Ooshima, A. Hase and Y. Kawamura, *Food Addit. Contam., Part A*, 2016, **33**, 1490–1498.
18 J. Soto-Alvaredo, M. Montes-Bayón and J. Bettmer, *Anal. Chem.*, 2013, **85**, 1316–1321.
19 B. Franze and C. Engelhard, *Anal. Chem.*, 2014, **86**, 5713–5720.
20 M. E. Hoque, K. Khosravi, K. Newman and C. D. Metcalfe, *J. Chromatogr. A*, 2012, **1233**, 109–115.
21 E. Bolea, J. Jiménez-Lamana, F. Laborda and J. R. Castillo, *Anal. Bioanal. Chem.*, 2011, **401**, 2723–2732.
22 F. Laborda, J. Jiménez-Lamana, E. Bolea and J. R. Castillo, *J. Anal. At. Spectrom.*, 2011, **26**, 1362–1371.
23 W.-C. Lee, B.-T. Lee, S. Lee, Y. S. Hwang, E. Jo, I.-C. Eom, S.-W. Lee and S.-O. Kim, *Microchem. J.*, 2016, **129**, 219–230.
24 K. A. Huynh, E. Siska, E. Heithmar, S. Tadjiki and S. A. Pergantis, *Anal. Chem.*, 2016, **88**, 4909–4916.
25 I. Strenge and C. Engelhard, *J. Anal. At. Spectrom.*, 2015, **31**, 135–144.
26 J. Liu, K. E. Murphy, R. I. MacCuspie and M. R. Winchester, *Anal. Chem.*, 2014, **86**, 3405–3414.
27 I. Abad-Álvaro, E. Peña-Vázquez, E. Bolea, P. Bermejo-Barrera, J. R. Castillo and F. Laborda, *Anal. Bioanal. Chem.*, 2016, **408**, 5089–5097.
28 F. Laborda, J. Jiménez-Lamana, E. Bolea and J. R. Castillo, *J. Anal. At. Spectrom.*, 2013, **28**, 1220–1232.
29 S. Lee, X. Bi, R. B. Reed, J. F. Ranville, P. Herckes and P. Westerhoff, *Environ. Sci. Technol.*, 2014, **48**, 10291–10300.
30 E. Caballero-Díaz, C. Pfeiffer, L. Kastl, P. Rivera-Gil, B. Simonet, M. Valcárcel, J. Jiménez-Lamana, F. Laborda and W. J. Parak, *Part. Part. Syst. Charact.*, 2013, **30**, 1079–1085.

